Article

Current Biology

H3.3 Nucleosome Assembly Mutants Display a Late-Onset Maternal Effect

Highlights

- Loss of H3.3 assembly factors results in late-onset defects
- Mitochondrial stress likely contributes to these late-onset defects
- The late-onset defects of H3.3 assembly mutants can be maternally rescued

Authors

Kirk B. Burkhart, Steven R. Sando, Anna Corrionero, H. Robert Horvitz

Correspondence

horvitz@mit.edu

In Brief

Burkhart *et al*. show that mutants lacking components of H3.3 assembly complexes have pleiotropic defects that manifest near the onset of adulthood. Mitochondrial stress likely contributes to these late-onset defects. The late-onset defects of H3.3 assembly mutants can be maternally rescued.

Burkhart et al., 2020, Current Biology *30*, 2343–2352
June 22, 2020
https://doi.org/10.1016/j.cub.2020.04.046

CellPress

Current Biology

CellPress

Article

H3.3 Nucleosome Assembly Mutants Display a Late-Onset Maternal Effect

Kirk B. Burkhart,[1] Steven R. Sando,[1] Anna Corrionero,[1,2] and H. Robert Horvitz[1,3,*]
[1]Howard Hughes Medical Institute, Department of Biology, Massachusetts Institute of Technology, Cambridge, MA 02139, USA
[2]Present address: Stoke Therapeutics, Bedford, MA 01730, USA
[3]Lead Contact
*Correspondence: horvitz@mit.edu
https://doi.org/10.1016/j.cub.2020.04.046

Maternally inherited RNA and proteins control much of embryonic development. The effect of such maternal information beyond embryonic development is largely unclear. Here, we report that maternal contribution of histone H3.3 assembly complexes can prevent the expression of late-onset anatomical, physiologic, and behavioral abnormalities of *C. elegans*. We show that mutants lacking *hira-1*, an evolutionarily conserved H3.3-deposition factor, have severe pleiotropic defects that manifest predominantly at adulthood. These late-onset defects can be maternally rescued, and maternally derived HIRA-1 protein can be detected in *hira-1(−/−)* progeny. Mitochondrial stress likely contributes to the late-onset defects, given that *hira-1* mutants display mitochondrial stress, and the induction of mitochondrial stress results in at least some of the *hira-1* late-onset abnormalities. A screen for mutants that mimic the *hira-1* mutant phenotype identified PQN-80—a HIRA complex component, known as UBN1 in humans—and XNP-1—a second H3.3 chaperone, known as ATRX in humans. *pqn-80* and *xnp-1* abnormalities are also maternally rescued. Furthermore, mutants lacking histone H3.3 have a late-onset defect similar to a defect of *hira-1*, *pqn-80*, and *xnp-1* mutants. These data demonstrate that H3.3 assembly complexes provide non-DNA-based heritable information that can markedly influence adult phenotype. We speculate that similar maternal effects might explain the missing heritability of late-onset human diseases, such as Alzheimer's disease, Parkinson's disease, and type 2 diabetes.

INTRODUCTION

Much of embryonic development is controlled by RNA and protein contributed by gametes to the zygote. The effect of this information is exemplified by maternal-effect mutants, which have been identified for a wide range of organisms, including, *C. elegans* [1], *Drosophila* [2], *Xenopus* [3], zebrafish [4], and mice [5]. For the vast majority of these mutants, animals that fail to inherit specific RNA from the oocyte have defects in embryonic development. If and how defects that manifest in adult animals can be maternally rescued is largely unknown. The elucidation of such maternal effects would be important for understanding the basic principles of inheritance and potentially important for understanding late-onset human disease.

Chromatin is assembled by histone chaperones. The histone cell cycle regulator (HIRA) complex and alpha-thalassemia/mental retardation X-linked (ATRX) are two evolutionarily conserved histone chaperones that facilitate the deposition of the histone variant H3.3 onto chromatin in a DNA-replication-independent process [6]. The HIRA complex consists of HIRA, ubinuclein 1 (UBN1), and calcineurin-binding protein 1 (CABIN1) [7]. This complex was first identified in *S. cerevisiae*, in which it represses histone gene transcription [8, 9] and has been shown to deposit H3.3 at gene bodies and regulatory elements in animal cells [10]. ATRX functions with death-associated protein 6 (DAXX) to deposit H3.3 at repetitive elements and telomeres [10]. Mutations in ATRX are the sole cause of ATRX syndrome [11], and mutations in ATRX and H3.3 can drive cancer formation [12–15]. Thus, H3.3-containing chromatin is important for essential cellular processes in eukaryotes, and mutations in components of these complexes drive human disease. Nonetheless, much of what is known about HIRA, ATRX, and H3.3 derives from studies of cell culture because loss of the HIRA complex, ATRX, or H3.3 results in embryonic lethality in many species [16–20]. We sought to understand the biological role of H3.3 assembly pathways by studying mutants that perturb this complex in *C. elegans* and discovered an unusual maternal effect: the inheritance of H3.3 assembly components via the maternal germline is sufficient to rescue defects that manifest near adulthood.

RESULTS

Loss of *hira-1* Results in Late-Onset Defects

Like most eukaryotic genomes, the *C. elegans* genome contains a single ortholog of *HIRA*, the gene *hira-1* (Figure 1A). To determine the normal biological role of *hira-1*, we examined the phenotype of a strain homozygous for a *hira-1* early premature termination mutation, allele *gk835598* (Figure 1B). Compared with adult wild-type animals, adult *gk835598* animals were small and pale (Figures 1C and S1A), defective in the enteric muscle contraction (EMC) that is the final step of the defecation motor program (Figure 1D), defective in pharyngeal pumping (Figure 1E), short-lived (Figure 1F), and reduced in fertility (Figure 1G). The size, pigmentation, and pumping defects were detectable in only adult animals (Figures 1C, S1A, and 1E), and the EMC defect was undetectable at the L1 larval stage and was minor until

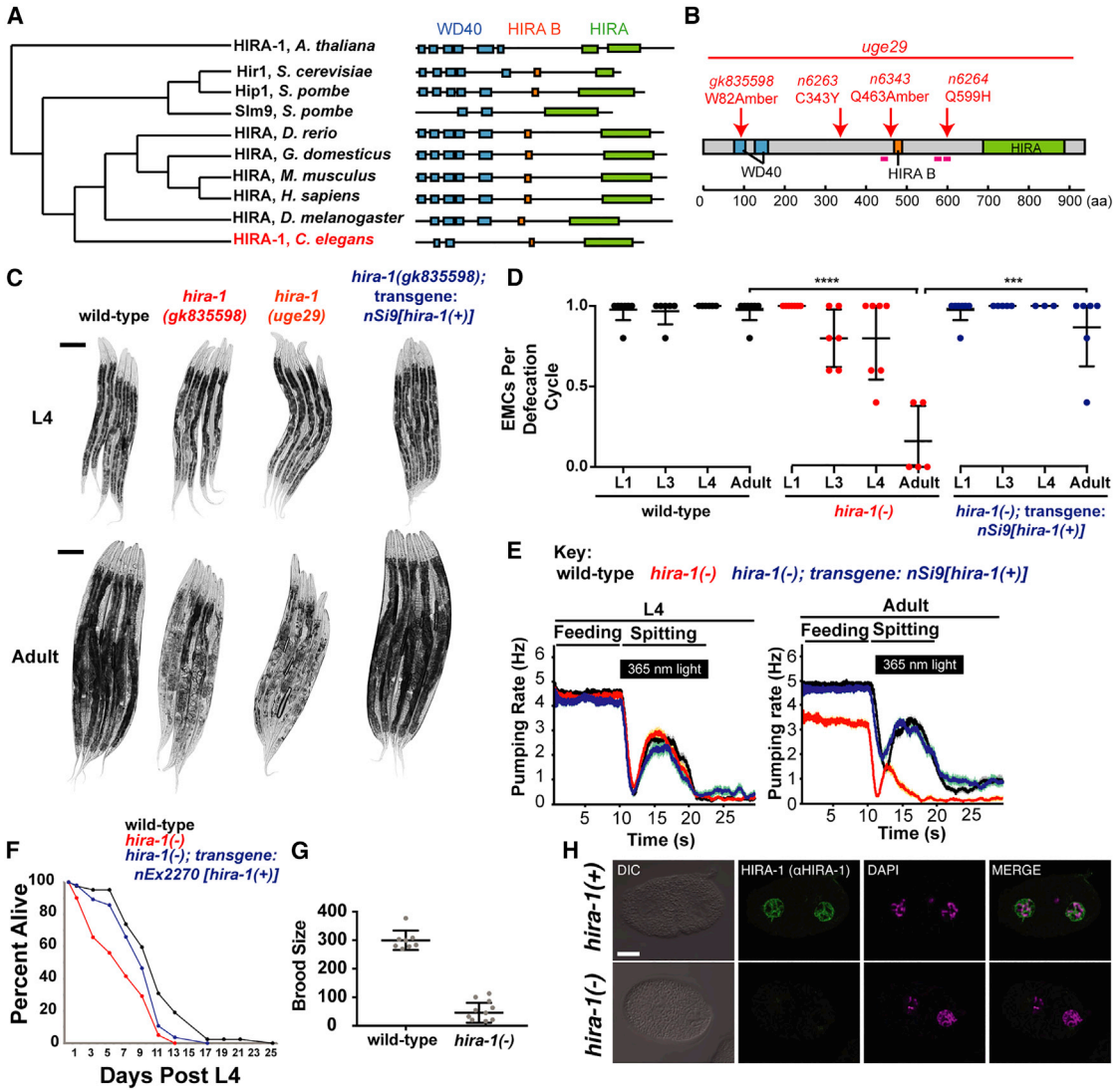

Figure 1. Loss of *hira-1* Results in Late-Onset Pleiotropic Defects

(A) Cladogram, adapted from TreeFam [22], of HIRA proteins in species indicated.

(B) HIRA-1 domain organization with mutant alleles indicated. Magenta lines indicate peptide sequences used to raise anti-HIRA-1 antibodies. Abbreviation is as follows: aa, amino acids.

(C) Micrographs of five representative animals of the indicated genotypes at the L4 larval and adult stages. Scale bars, 100 μm.

(D) Fraction of defecation cycles with an EMC in animals of the indicated genotypes at the indicated stages. Each data point represents a single animal for which five defecation cycles were scored; N ≥ 3, mean ± SD.

(E) The pharyngeal feeding and light-evoked spitting behaviors of animals of the indicated genotypes and stages. The pharyngeal contraction (i.e., "pumping") rate as a moving average is shown (N = 60 animals).

(F) Survival curves for animals of the indicated genotypes N ≥ 41.

(G) The number of progeny produced by animals of the indicated genotypes; N ≥ 8, mean ± SD.

(H) Micrographs of wild-type and *hira-1(gk835598)* mutant 2-cell embryos stained with DAPI (magenta) and anti-HIRA-1 (green) antibody (rabbit 39215). Scale bar, 10 μm.

See also Figure S1. *hira-1(–)* refers to the *gk835598* allele. **p ≤ 0.01, ***p ≤ 0.001, ****p ≤ 0.0001 by Student's t test.

adulthood (Figure 1D). Three lines of evidence indicate that these defects were caused by loss of *hira-1* function and most likely the null phenotype: (1) a strain with a deletion allele (*uge29*) [21] eliminating *hira-1* mimicked the *gk835598* strain for all aspects of the *hira-1(gk835598)* phenotype tested (Figures 1C and S1A); (2) HIRA-1 protein as detected by immunofluorescence using two different antibodies raised against HIRA-1 was abolished in *gk835598* embryos (Figures 1H and S1B); and (3) introducing a wild-type copy of the *hira-1* gene into *hira-1(gk835598)* mutants rescued all of these defects (Figures 1C, S1A, and 1D–1F). Altogether, these data indicate that loss of *hira-1* results in pleiotropic defects that are minor or undetectable until adulthood

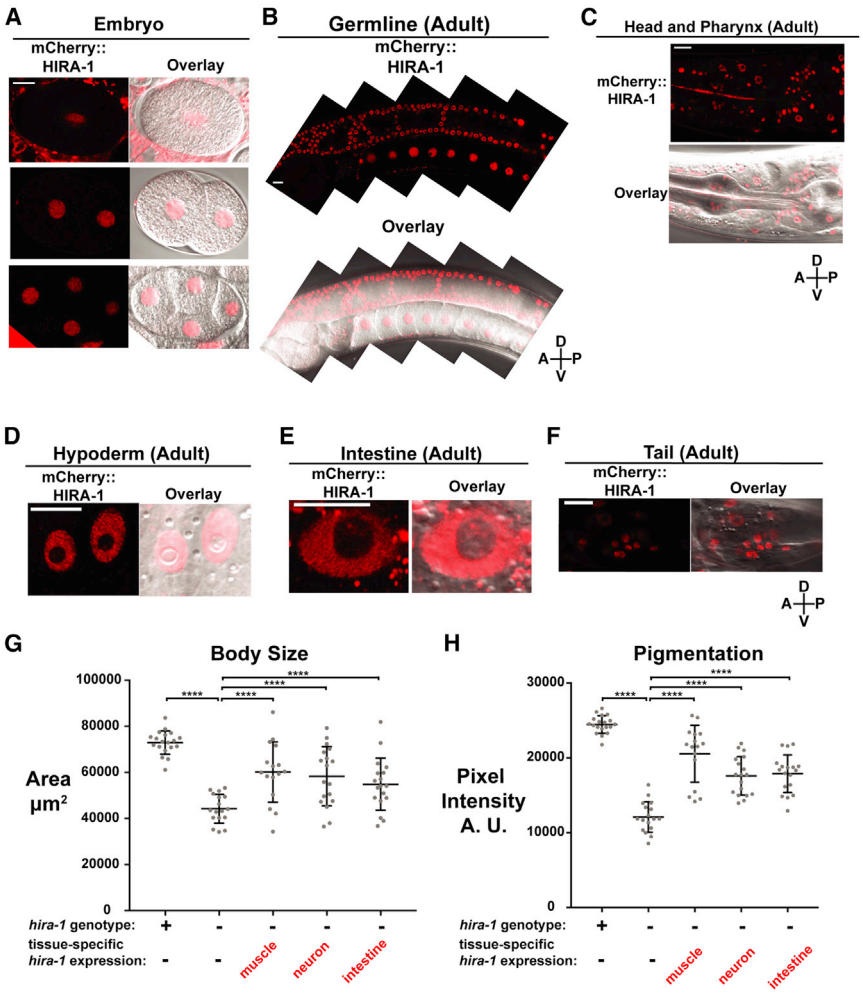

Figure 2. HIRA-1 Is Broadly Expressed and Can Function in Multiple Cell Types

(A–F) Representative fluorescent and fluorescent-DIC overlay micrographs of mCherry::HIRA-1 expressed from a single-copy integrated transgene (*nSi48:P*$_{hira-1}$*::mCherry::hira-1*) in (A) embryos, (B) the adult germline, (C), the adult pharynx, (D) adult hypoderm nuclei in hyp7, (E) adult intestinal nuclei, and (F) the adult tail. mCherry::HIRA-1 shows diffuse nuclear localization but is largely omitted from the nucleolus.

(G and H) Wild-type animals, *hira-1*$^{-}$ animals, and *hira-1*$^{-}$ animals expressing transgenes driving *hira-1*$^{+}$ expression in muscle (*nEx2902*), neurons (*nEx2892*), or intestine (*nEx2897*) were scored for (G) body size and (H) pigmentation; mean ± SD. See also Figure S2.

Scale bars, 10 µm. *hira-1(–)* refers to the *gk835598* allele. ****p ≤ 0.0001 by Student's t test.

and therefore will be referred to as "late-onset." These data suggest that *hira-1* is largely not needed for normal embryonic and larval development but rather is specifically needed for the normal physiology of adult animals.

HIRA-1 Can Act in Multiple Cell Types

To determine the cell types in which HIRA-1 acts to prevent these late-onset pleiotropic defects, we first examined the expression pattern of *hira-1*. We generated transgenic animals that express *mcherry::hira-1* under the *hira-1* promoter from a single-copy transgene integrated in the genome. This transgene was able to rescue *hira-1* mutant defects (Figure S2A) and was detectable in many, if not all, cells throughout development and in adults (Figures 2A–2F). Next, we generated transgenic *hira-1(–)* lines that express *hira-1(+)* in a tissue-specific manner using promoters that drive expression in the intestine, muscle, or neurons (Figure S2B). The small, pale, and pharyngeal pumping defects of *hira-1* mutants were partially rescued by driving *hira-1(+)* expression in the intestine, muscle, or neurons (Figures S2C, 2G, 2H, and S2D) indicating that *hira-1* can function in multiple cell types. Given the broad *hira-1* expression pattern, we suggest that *hira-1* normally promotes a cell non-autonomous process that originates broadly through the animal and in at least intestinal cells, muscle, and neurons. The EMC defect was partially rescued by driving *hira-1(+)* expression in neurons and intestine but not muscle (Figure S2E), suggesting *hira-1* normally functions in intestine and neurons but not muscle to maintain normal defecation behavior.

Because *hira-1* can function in intestinal cells, muscle, or neurons, we examined intestinal cells (which are easy to score) in *hira-1* mutant larvae and adults. These mutants had a normal number of intestinal nuclei in both larvae and adults (Figure S2F). However, the morphology of some intestinal nuclei was abnormal in adults (Figures S2G and S2H). These data further suggest that embryonic and larval development are normal in *hira-1* mutants and that the late-onset defects are occurring at the cellular level.

Maternally Contributed HIRA-1 Rescues Late-Onset Defects

During backcrosses with *hira-1* mutants, we observed that the late-onset pleiotropies were parentally rescued. To confirm and quantify this finding, we examined *hira-1(–/–)* animals generated by *hira-1(+/–)* hermaphrodite parents; these *hira-1(–/–)* animals were indistinguishable from wild-type animals with respect to the small, pale, and defecation defects (Figures 3A, S3A, S3B, and 3B), indicating that the late-onset defects of *hira-1* mutants were parentally rescued. To determine whether *hira-1* mutant defects were paternally or maternally rescued (or both), we analyzed *hira-1(–/–)* progeny generated by *hira-1(–/–)* hermaphrodites crossed with *hira-1(+/–)* fathers (Figure 3C). These animals still had the small, pale, and defecation defects (Figures 3C, S3C, S3D, and 3D), indicating that *hira-1* mutant defects were not paternally rescued. Furthermore, *hira-1(+/–)* progeny generated from *hira-1(–/–)* mothers and *hira-1(+/–)* fathers did not have the small, pale, or defecation defects (Figures 3C, S3C, S3D, and 3D), indicating that *hira-1* mutant defects were zygotically rescued. The brood-size defect of *hira-1*

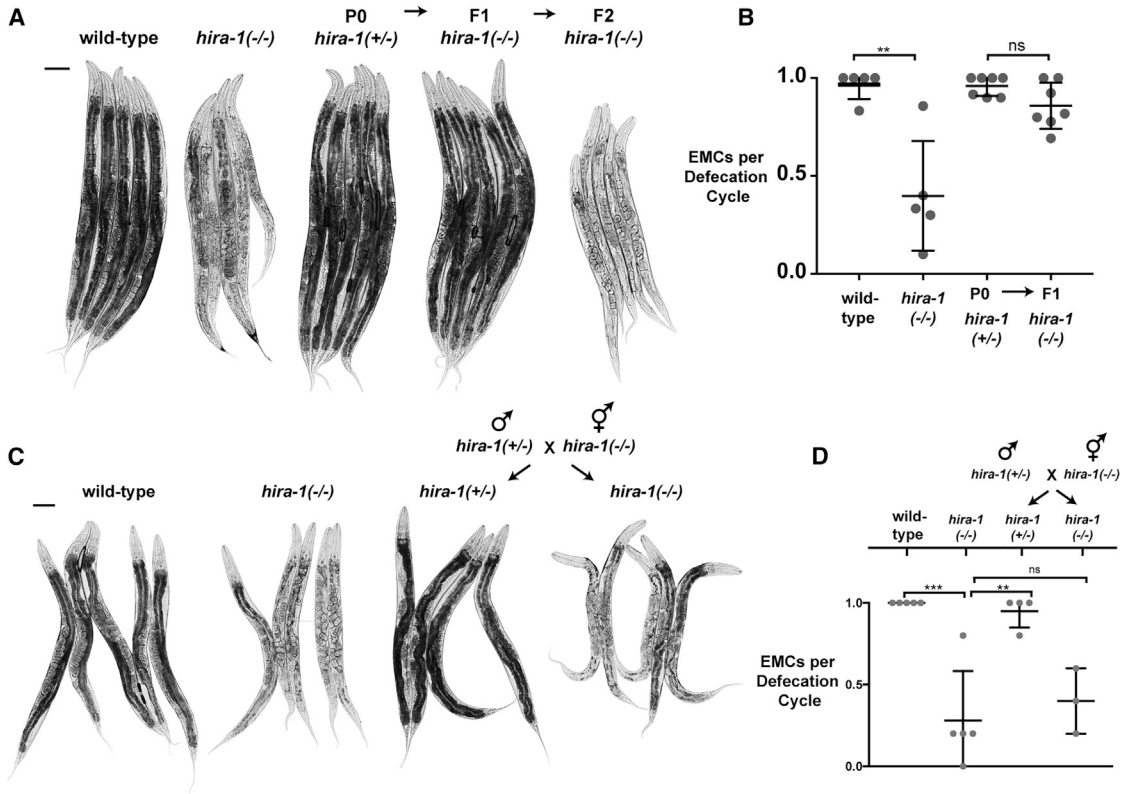

Figure 3. The Late-Onset Defects of *hira-1* Mutants Are Maternally Rescued

(A) Micrographs of five representative adult animals of the indicated genotypes and generations. *hira-1(+/−)* signifies *hira-1(gk835598) / qC1*. *qC1* is a balancer chromosome (carrying *hira-1(+)*) that suppresses recombination on the left arm of chromosome III and was used to maintain the *hira-1(gk835598)* mutation in heterozygotes [23]. Scale bar, 100 μm.

(B) Fraction of EMCs per defecation cycle of adult animals of the indicated genotypes and generations; N = 5, mean ± SD.

(C) Micrographs of representative adult control animals (wild-type and *hira-1*$^{-}$) and adult progeny of the indicated genotype from the indicated cross. Scale bar, 100 μm. Males from the indicated cross carry an X-linked *gfp* (*ccIs4810: lmn-1::gfp*) to identify cross progeny hermaphrodites. *hira-1(+/−)* signifies *hira-1(gk835598) / qC1*.

(D) Fraction of EMCs per defecation cycle of adult animals of the indicated genotypes as in (C). Males from the indicated cross carry an X-linked *gfp* (*ccIs4810: lmn-1::gfp*) to identify cross progeny hermaphordites. *hira-1(+/−)* signifies *hira-1(gk835598) / qC1*.; N ≥ 3, mean ± SD. **p ≤ 0.01, ***p ≤ 0.001 by Student's t test.

See also Figure S3.

mutants was not parentally rescued (Figure S3E). Consistent with the maternal rescue of *hira-1* mutants, mCherry::HIRA-1 protein was detectable in embryos and adults that did not carry this transgene in their genomes but were generated by mothers heterozygous for the transgene (Figures S3F, S3G, and S3H). To detect maternally derived HIRA-1 in adults, we needed to increase the intensity of the laser and exposure to amounts that saturate the signal of the non-maternally derived control. Thus, the maternally derived HIRA-1 protein in adults was barely detectable and far lower than that seen at earlier stages. In addition, we detected HIRA-1 protein in mature oocytes and embryos prior to zygotic activation (Figures 1H, 2A, and 2B). These data indicate that HIRA-1 (mRNA or protein) can be inherited via the maternal germline and that inherited HIRA-1 can rescue late-onset defects of *hira-1* mutants.

Loss of *hira-1* Results in Chronic Mitochondrial Stress

To better understand the molecular defects of *hira-1* mutants, we performed RNA-sequencing (RNA-seq) of wild-type and *hira-1* mutants at three developmental stages: L1, L4, and adult. Although *hira-1* mutant abnormalities predominantly manifested at the onset of adulthood, we were able to detect significant gene expression changes in *hira-1* mutants prior to the onset of adulthood (stages L1 and L4) (Figure 4A; Table S1), suggesting that the chronic misexpression of genes over time might result in the late-onset defects. We focused on chronically misexpressed genes, namely genes that were misexpressed in the same direction in all three stages (77 genes) (Figures 4B dotted line, S4A, and S4B). Using WormExp [24], we compared the chronically misexpressed genes with 2,293 previously published *C. elegans* gene expression profiles from studies of a broad range of biological contexts. Six of the top 15 hits from this analysis were from animals undergoing mitochondrial insults (Figure S4C). That *hira-1* mutants have a gene-expression profile similar to those of animals undergoing mitochondrial insults suggested that *hira-1* mutants are experiencing mitochondrial stress. Supporting this hypothesis, we observed that *hira-1* mutants showed activation of two different reporters of mitochondrial stress ($P_{hsp\text{-}6}$*::gfp* and

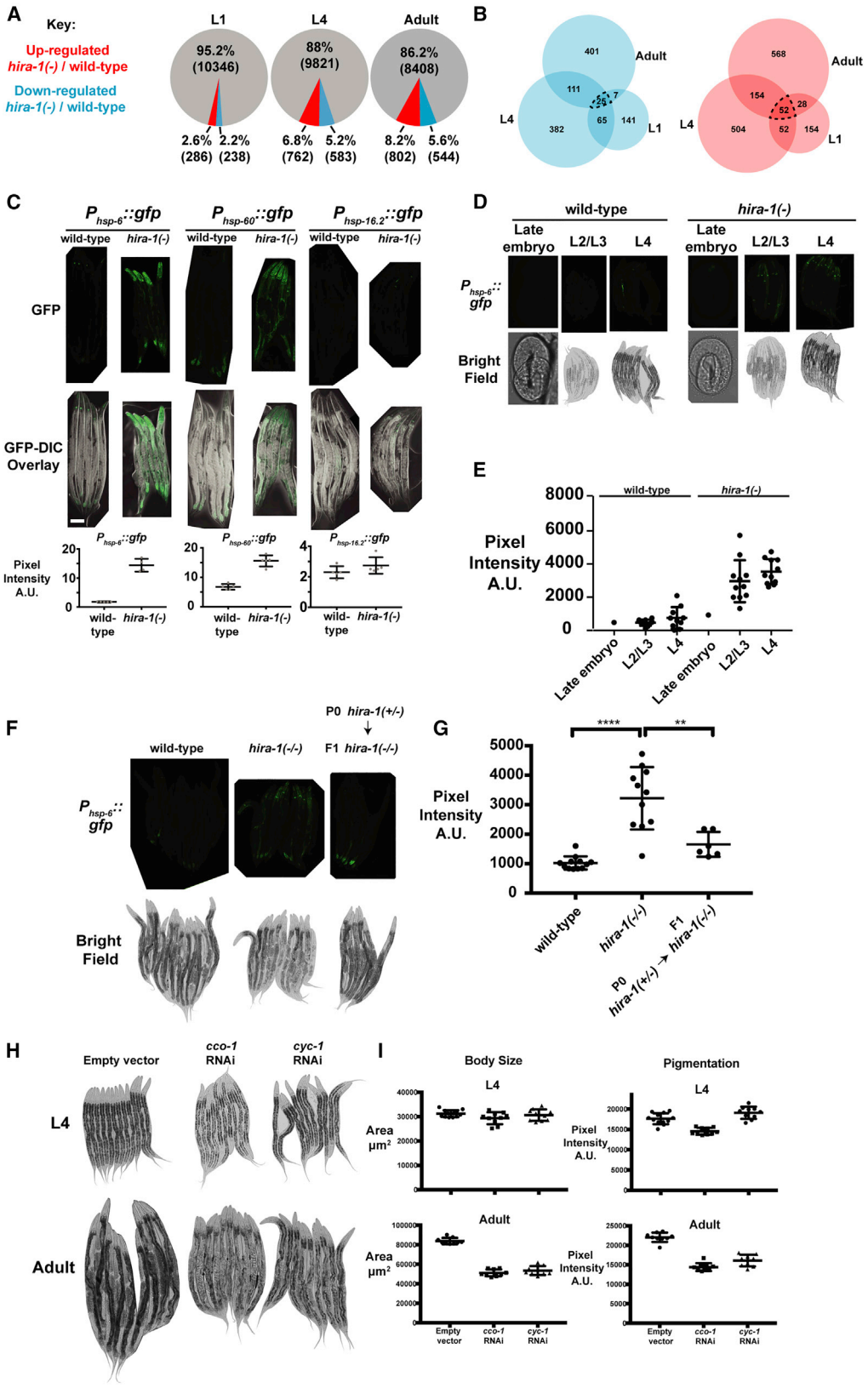

(legend on next page)

P_{hsp-60}*::gfp*) but no activation of a reporter for the cytosolic heat-shock response ($P_{hsp-16.2}$*::gfp*) (Figure 4C). The mitochondrial stress response was activated throughout development (Figures 4D and 4E). Like the late-onset defects of *hira-1* mutants, activation of the mitochondrial stress response was maternally rescued (Figures 4F and 4G). Thus, loss of *hira-1* results in chronic activation of the mitochondrial stress response. Others have reported that mitochondrial stress can result in animals that have late-onset small and pale defects [25–27], like *hira-1* mutants. Similarly, we found that RNAi targeting *cco-1* and *cyc-1* (two different mitochondrial components) led to late-onset small and pale defects (Figures 4H and 4I). We conclude that mitochondrial stress likely drives at least some aspects of the late-onset defects of *hira-1* mutants.

Loss of *hira-1* Results in Upregulation of Histone Gene Expression

We noted that 25% (13 out of 52) of the chronically upregulated genes in *hira-1* mutants encode histones (Figure S4A); that of the 39 histone genes with expression amounts we were able to detect, 35 were upregulated in at least one developmental stage (Figure S4D); and that on average histone gene expression in *hira-1* adults was 11-fold higher than in wild-type animals (with a median of 26-fold higher) (Figure S4D). The number of histones we were able to detect was limited by the high sequence identity shared by histone genes, which leads to difficulty in unambiguously mapping reads to individual histone genes. Our RNA-seq analysis was done on polyA-selected RNA. Mangone et al. [28] identified polyadenylation of transcripts of most histone genes in *C. elegans*. Thirty-five of the 39 histone genes we detected as expressed were found to be polyadenylated in this paper. We conclude that loss of *hira-1* results in a striking upregulation of histone gene expression. In yeast, the Hir complex assembles nucleosomes at histone gene promoters to repress histone gene expression outside of S-phase [8, 9, 29]. We propose that in *C. elegans* HIRA-1 plays a similar role in repressing histone gene expression. Alternatively, it is possible that a failure to assemble nucleosomes in *hira-1* mutants causes cells to compensate and upregulate histone gene expression.

A Screen for Mutants Similar to *hira-1* Mutants Identified Components of H3.3 Chromatin Assembly Complexes

To better understand why *hira-1* function is needed for diverse late-stage characteristics, we sought other genes that function similarly to *hira-1*. We performed an EMS mutagenesis screen for mutants that, like *hira-1* mutants, are small, pale, and misexpress P_{hsp-6}*::gfp* (a mitochondrial stress reporter activated in *hira-1* mutants) (Figures S5A and 4C). We reasoned that by using these three aspects of the *hira-1* phenotype to screen, we would specifically enrich for mutants similar to *hira-1* mutants. We screened in the F3 generation, because these mutant defects are maternally rescued. We identified three new alleles of *hira-1* (Figures 5A, 1B, and S5B), validating the screen and confirming our phenotypic analyses. We also identified a deletion allele of *pqn-80* (Figures 5A–5C). Interpro [30] analysis of the PQN-80 sequence identified a HRD domain (Figures S5C and 5C). The HRD domain is defined by a core member of the HIRA complex known as UBN1 in humans and histone promoter control protein 2 (HPC2) in yeast [31]. We propose that PQN-80 is the *C. elegans* ortholog of UBN1 and HPC2. Our screen also identified four alleles of the ATRX homolog gene *xnp-1* (Figures 5A, 5B, S5B, and 5E). *pqn-80* and *xnp-1* mutants had maternally rescued small and pale defects similar to those of *hira-1* mutants (Figure 5A, 5B, and S5B). Additionally, like *hira-1* mutants, *pqn-80* and *xnp-1* mutants had late-onset defects in defecation (Figures 5D and 5F). In short, *pqn-80* and *xnp-1* mutants are nearly identical in phenotype to *hira-1* mutants. In *Drosophila*, Hira and Xnp can be recruited to the same genomic sites [32]. Given the similarities of phenotypes of *hira-1* and *xnp-1* mutants, we propose that the misregulation of common targets leads to similar phenotypic defects.

The HIRA complex and ATRX have well-established roles as H3.3 chaperones. We next asked whether animals lacking H3.3 share abnormalities with *hira-1*, *pqn-80*, and *xnp-1* mutants. *C. elegans* has five H3.3-like genes [34]. A quintuple mutant lacking all five H3.3 genes [21] did not have defects in body size or pigmentation (Figure S5D) but did have a late-onset defect in defecation (Figure 5G). A similar defect was produced by RNAi against the H3.3 gene *his-72* (Figure 5H). We also observed activation of a mitochondrial stress reporter after RNAi against *his-72* (Figure S5E). The difference between the defects observed in the H3.3 assembly factor mutants and the H3.3 mutant might be explained by the ability of H3 to compensate for loss of H3.3, a phenomenon observed for *Drosophila* [35].

Our data establish that mutants lacking components of H3.3 assembly complexes have maternally rescued late-onset defects at least some of which are likely caused by mitochondrial stress.

Figure 4. Loss of *hira-1* Results in Chronic Activation of the Mitochondrial Stress Response

(A) Genes that change expression in *hira-1(−)* compared with those in wild-type animals. Color coding is as follows: red, genes upregulated (at least 2-fold, $p < 0.01$); blue, genes downregulated (at least 2-fold, $p < 0.01$); gray, all other genes.

(B) Venn diagrams representing overlap between genes downregulated at the indicated stages (blue) and overlap between genes upregulated in the indicated stages (red).

(C) Top row, fluorescent micrographs of five representative adults of the indicated genotypes expressing the indicated stress reporters. In the middle row are GFP-DIC overlay micrographs of the animals imaged above. In the bottom row is a quantification of the GFP signal from animals above; $N \geq 4$, mean ± SD.

(D) P_{hsp-6}*::gfp* fluorescence (top) and bright-field (bottom) micrographs of embryos or animals of the indicated genotypes at the indicated stages.

(E) Quantification of the GFP signal from embryos and animals in (D); mean ± SD.

(F) P_{hsp-6}*::gfp* fluorescence (top) and bright-field (bottom) micrographs of adults of the indicated genotypes and generation.

(G) Quantification of GFP signal from animals in (F); mean ± SD.

(H) Micrographs of 9–12 representative wild-type animals of the indicated stages undergoing RNAi to the indicated genes or no RNAi (empty vector).

(I) Quantification of the body size and pigmentation of the animals imaged in (H); mean ± SD.

See also Figure S4 and Table S1. *hira-1(−)* refers to the *gk835598* allele. $^{**}p \leq 0.01$, $^{****}p \leq 0.0001$ by Student's t test.

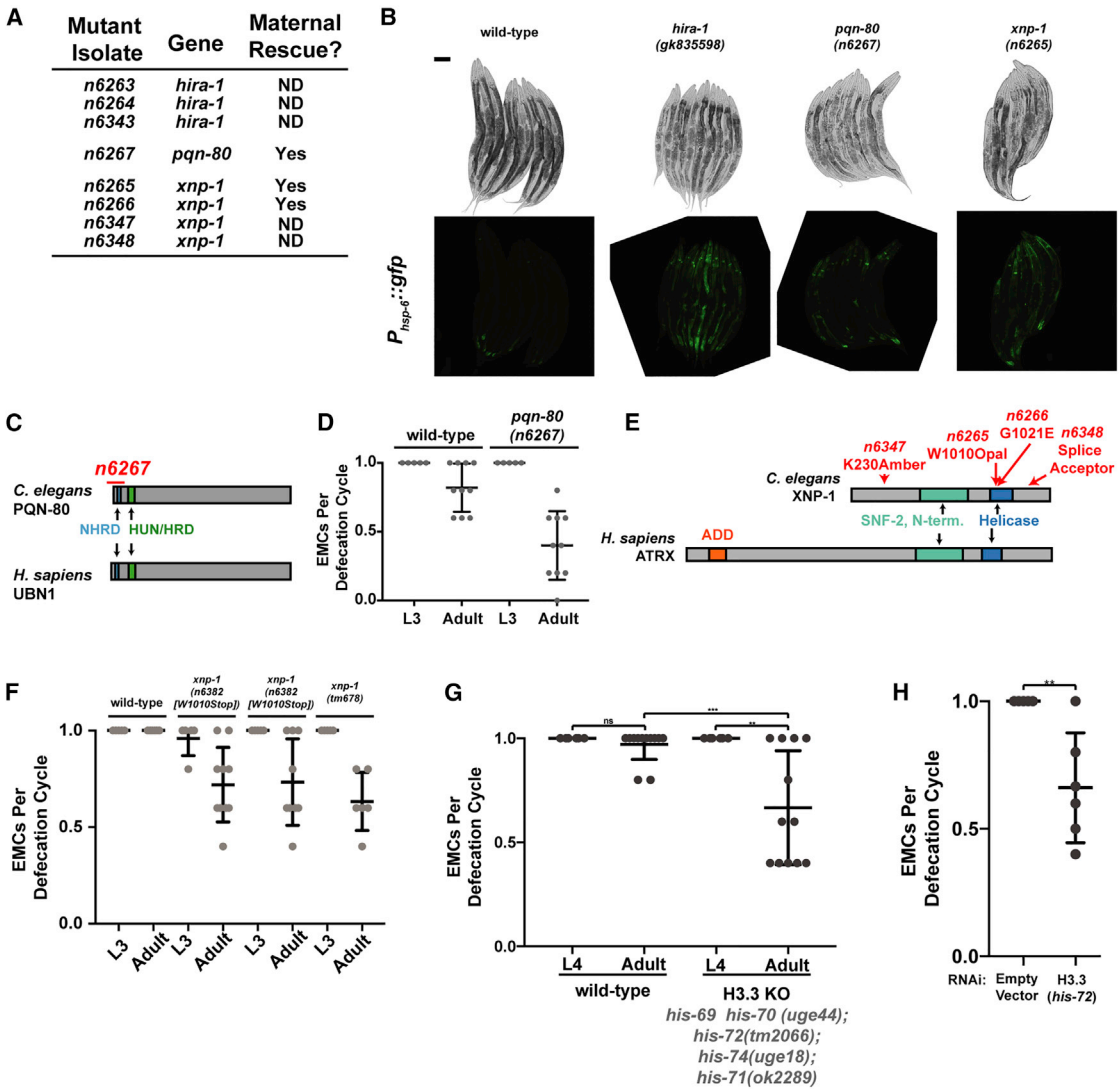

Figure 5. A Screen for Mutants That Mimic *hira-1* Mutants Identified Components of H3.3 Chromatin Assembly Complexes

(A) Some of the mutant isolates identified in the screen. ND, not determined.

(B) Bright-field (top) and $P_{hsp\text{-}6}$*::gfp* fluorescence (bottom) micrographs of 8–10 representative animals of the indicated genotypes.

(C) Domain organization of *C. elegans* PQN-80 and human UBN1, showing the *n6267* deletion allele of *pqn-80* identified from the screen (red).

(D) Fraction of defecation cycles with an EMC in animals of the indicated genotypes at the indicated developmental stages. These strains contain $P_{hsp\text{-}6}$*::gfp*. N ≥ 5, mean ± SD.

(E) Domain organizations of *C. elegans* XNP-1 and human ATRX showing alleles of *xnp-1* identified in the screen (red). ADD is an H3-binding module to which binding is promoted by H3 lysine 9 trimethylation [33].

(F and G) Fraction of defecation cycles with an EMC was scored in animals of the indicated genotypes at the indicated developmental stages; N ≥ 5, mean ± SD.

(H) Fraction of defecation cycles with an enteric muscle contraction in wild-type adult animals exposed to dsRNA targeting the indicated gene; N ≥ 5, mean ± SD.

**p ≤ 0.01, ***p ≤ 0.001 by Student's t test.

See also Figure S5. Scale bars, 100 μm

DISCUSSION

Whereas most maternal-effect mutants have defects in embryonic development [1–5], mutants in *hira-1*, *pqn-80*, and *xnp-1* have maternally rescued defects that manifest near the onset of adulthood. Embryonic and larval development are largely normal in these H3.3 assembly mutants, but near the onset of adulthood there appears to be a failure of multiple cell types. We propose that chronic mitochondrial stress drives much of this cellular dysfunction and that the inheritance of H3.3 assembly factors via the maternal germline is sufficient to provide lifelong protection from mitochondrial stress (Figure 6).

H3.3 Assembly Mutants Display a Prolonged Maternal Effect

The defects of H3.3 assembly mutants in body size, pigmentation, pharyngeal pumping, and defecation are minor or undetectable until adulthood, suggesting that the cells that control these

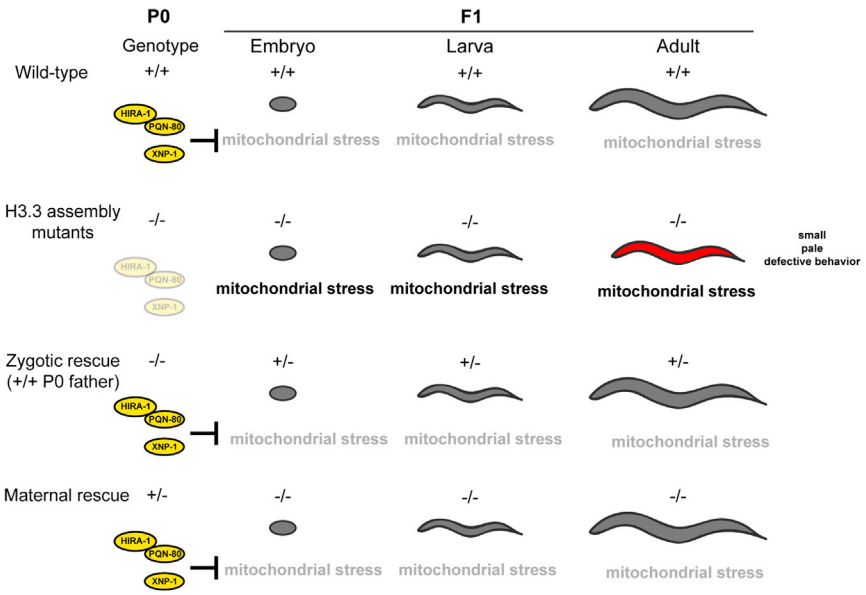

Figure 6. Maternal H3.3 Assembly Complexes Are Sufficient to Prevent Late-Onset Defects

Loss of H3.3 assembly factors results in pleiotropic defects that manifest near the onset of adulthood. These defects are likely caused by chronic mitochondrial stress. Inheriting these factors through the maternal germline is sufficient to rescue these late-onset defects.

processes develop and function normally in the embryo and larvae. Consistent with this view, we observed that intestinal cells (in which *hira-1* can act to rescue the late-onset defects) did not display any obvious developmental abnormalities in embryos or larvae but did become morphologically abnormal in adults. We propose that the late-onset defects of H3.3 assembly mutants are not caused by embryonic or larval developmental defects but rather by late-onset cellular dysfunction. We note that maternal effects that impact stages after embryonic development have been described for *C. elegans* [36, 37], snails [38], zebrafish [39], and mice [40], indicating the impact of maternal effects on later life stages can occur in a range of organisms.

What Is the Mechanism behind the Long-Lasting Maternal Effect?

Mechanistically, how might maternally contributed HIRA-1 prevent mitochondrial stress throughout embryonic development and into adulthood? We were able to detect maternally derived HIRA-1 in adult animals. Although the amount in adults appeared to be far lower than that in embryos, it is conceivable that the maternally derived protein that persists into adults is sufficient to rescue the late-onset defects. We prefer an alternative hypothesis—maternally derived HIRA-1 establishes in embryos a chromatin state that can persist into adult animals. H3.3 and its assembly factors are maternally contributed in *Drosophila* [16], *Xenopus* [41], and mice [17, 42, 43]. HIRA and ATRX have been shown to deposit H3.3 onto chromatin in embryonic stem cells [44–46] and during early embryonic development in *Drosophila* [16], *Xenopus* [41], and mice [17, 47, 48]. After somatic nulcei are implanted into enucleated eggs of *Xenopus*, H3.3 is needed for maintaining an epigenetic memory of gene expression that can persist through 24 mitotic divisions [49]. We speculate that epigenetic states established by the deposition of H3.3 in the early embryo affect gene expression throughout much of the lifespan of many organisms and that this altered gene expression can affect phenotype later in life.

Parental Effects on Late-Onset Disease Might Be Underappreciated

Although a parental effect can impact lifespan in *C. elegans* [50] and a paternal effect can impact cancer formation in adult mice [51], relative to maternal effects that affect early embryonic development, parental effects that impact phenotypes that manifest at adulthood appear to be rare. Much of the heritability of many late-onset diseases—including type 2 diabetes, Alzheimer's, Parkinson's, and cancer—cannot be explained by changes in DNA sequence. We speculate that parental effects might be underappreciated in our understanding of the genetics of these and other human diseases in which the phenotypic effect of non-inherited alleles is often ignored [52].

STAR★METHODS

Detailed methods are provided in the online version of this paper and include the following:

- KEY RESOURCES TABLE
- RESOURCE AVAILABILITY
  - Lead Contact
  - Materials Availability
  - Data and Code Availability
- EXPERIMENTAL MODEL AND SUBJECT DETAILS
- METHOD DETAILS
  - Microscopy
  - Plasmid and transgenic strain construction
  - Defecation
  - Genetic screen and mutation identification
  - Pharyngeal pumping
  - Antibody production
  - RNA-Seq
  - Quantification of body size and pigmentation
- QUANTIFICATION AND STATISTICAL ANALYSIS

SUPPLEMENTAL INFORMATION

Supplemental Information can be found online at https://doi.org/10.1016/j.cub.2020.04.046.

ACKNOWLEDGMENTS

We thank A. Doi, N. Burton, C. Pender, C. Engert, V. Dwivedi, N. Bhatla, S. Luo, and other members of the Horvitz laboratory for discussions; F. Steiner for

sharing strains; and the *Caenorhabditis* Genetic Center, which is funded by the NIH Office of Research Infrastructure Programs (P40 OD010440) for strains. K.B. was supported by the Life Sciences Research Foundation (sponsored by Sanofi). This work was supported by NIH grant R01GM024663. H.R.H. is the David H. Koch Professor of Biology at MIT and an Investigator at the Howard Hughes Medical Institute.

AUTHOR CONTRIBUTIONS

Conceptualization, K.B. and H.R.H.; Methodology, K.B., S.S., and A.C.; Investigation K.B., S.S., and A.C; Writing – Original Draft, K.B. and H.R.H.; Funding Acquisition, K.B. and H.R.H.; Resources, K.B. and H.R.H.; Supervision, H.R.H.

DECLARATION OF INTERESTS

The authors declare no competing interests.

Received: January 6, 2020
Revised: March 31, 2020
Accepted: April 20, 2020
Published: May 28, 2020

REFERENCES

1. Bowerman, B. (1998). Maternal control of pattern formation in early *Caenorhabditis elegans* embryos. Curr. Top. Dev. Biol. *39*, 73–117.
2. Luschnig, S., Moussian, B., Krauss, J., Desjeux, I., Perkovic, J., and Nüsslein-Volhard, C. (2004). An F1 genetic screen for maternal-effect mutations affecting embryonic pattern formation in *Drosophila melanogaster*. Genetics *167*, 325–342.
3. Droin, A. (1992). The developmental mutants of *Xenopus*. Int. J. Dev. Biol. *36*, 455–464.
4. Dosch, R. (2015). Next generation mothers: Maternal control of germline development in zebrafish. Crit. Rev. Biochem. Mol. Biol. *50*, 54–68.
5. Condic, M.L. (2016). The Role of Maternal-Effect Genes in Mammalian Development: Are Mammalian Embryos Really an Exception? Stem Cell Rev Rep *12*, 276–284.
6. Hammond, C.M., Strømme, C.B., Huang, H., Patel, D.J., and Groth, A. (2017). Histone chaperone networks shaping chromatin function. Nat. Rev. Mol. Cell Biol. *18*, 141–158.
7. Ricketts, M.D., and Marmorstein, R. (2017). A molecular prospective for HIRA complex assembly and H3.3-specific histone chaperone function. J. Mol. Biol. *429*, 1924–1933.
8. Xu, H., Kim, U.J., Schuster, T., and Grunstein, M. (1992). Identification of a new set of cell cycle-regulatory genes that regulate S-phase transcription of histone genes in Saccharomyces cerevisiae. Mol. Cell. Biol. *12*, 5249–5259.
9. Osley, M.A., and Lycan, D. (1987). Trans-acting regulatory mutations that alter transcription of *Saccharomyces cerevisiae* histone genes. Mol. Cell. Biol. *7*, 4204–4210.
10. Grover, P., Asa, J.S., and Campos, E.I. (2018). H3-H4 Histone Chaperone Pathways. Annu. Rev. Genet. *52*, 109–130.
11. Gibbons, R.J., and Higgs, D.R. (2000). Molecular-clinical spectrum of the ATR-X syndrome. Am. J. Med. Genet. *97*, 204–212.
12. Dyer, M.A., Qadeer, Z.A., Valle-Garcia, D., and Bernstein, E. (2017). ATRX and DAXX: Mechanisms and Mutations. Cold Spring Harb. Perspect. Med. *7*, a026567.
13. Schwartzentruber, J., Korshunov, A., Liu, X.-Y., Jones, D.T.W., Pfaff, E., Jacob, K., Sturm, D., Fontebasso, A.M., Quang, D.-A.K., Tönjes, M., et al. (2012). Driver mutations in histone H3.3 and chromatin remodelling genes in paediatric glioblastoma. Nature *482*, 226–231.
14. Wu, G., Broniscer, A., McEachron, T.A., Lu, C., Paugh, B.S., Becksfort, J., Qu, C., Ding, L., Huether, R., Parker, M., et al.; St. Jude Children's Research Hospital–Washington University Pediatric Cancer Genome Project (2012). Somatic histone H3 alterations in pediatric diffuse intrinsic pontine gliomas and non-brainstem glioblastomas. Nat. Genet. *44*, 251–253.
15. Behjati, S., Tarpey, P.S., Presneau, N., Scheipl, S., Pillay, N., Van Loo, P., Wedge, D.C., Cooke, S.L., Gundem, G., Davies, H., et al. (2013). Distinct H3F3A and H3F3B driver mutations define chondroblastoma and giant cell tumor of bone. Nat. Genet. *45*, 1479–1482.
16. Loppin, B., Bonnefoy, E., Anselme, C., Laurençon, A., Karr, T.L., and Couble, P. (2005). The histone H3.3 chaperone HIRA is essential for chromatin assembly in the male pronucleus. Nature *437*, 1386–1390.
17. Lin, C.J., Koh, F.M., Wong, P., Conti, M., and Ramalho-Santos, M. (2014). Hira-mediated H3.3 incorporation is required for DNA replication and ribosomal RNA transcription in the mouse zygote. Dev. Cell *30*, 268–279.
18. Wang, M.Y., Guo, Q.H., Du, X.Z., Zhou, L., Luo, Q., Zeng, Q.H., Wang, J.L., Zhao, H.B., and Wang, Y.F. (2014). HIRA is essential for the development of gibel carp. Fish Physiol. Biochem. *40*, 235–244.
19. Garrick, D., Sharpe, J.A., Arkell, R., Dobbie, L., Smith, A.J.H., Wood, W.G., Higgs, D.R., and Gibbons, R.J. (2006). Loss of Atrx affects trophoblast development and the pattern of X-inactivation in extraembryonic tissues. PLoS Genet. *2*, e58.
20. Tang, M.C.W., Jacobs, S.A., Mattiske, D.M., Soh, Y.M., Graham, A.N., Tran, A., Lim, S.L., Hudson, D.F., Kalitsis, P., O'Bryan, M.K., et al. (2015). Contribution of the two genes encoding histone variant h3.3 to viability and fertility in mice. PLoS Genet. *11*, e1004964.
21. Delaney, K., Mailler, J., Wenda, J.M., Gabus, C., and Steiner, F.A. (2018). Differential expression of histone H3.3 genes and their role in modulating temperature stress response in *Caenorhabditis elegans*. Genetics *209*, 551–565.
22. Li, H., Coghlan, A., Ruan, J., Coin, L.J., Hériché, J.-K., Osmotherly, L., Li, R., Liu, T., Zhang, Z., Bolund, L., et al. (2006). TreeFam: a curated database of phylogenetic trees of animal gene families. Nucleic Acids Res. *34*, D572–D580.
23. Edgley, M.L., Baillie, D.L., Riddle, D.L., and Rose, A.M. (2006). Genetic balancers. WormBook, 1–32.
24. Yang, W., Dierking, K., and Schulenburg, H. (2016). WormExp: a web-based application for a *Caenorhabditis elegans*-specific gene expression enrichment analysis. Bioinformatics *32*, 943–945.
25. Dillin, A., Hsu, A.-L., Arantes-Oliveira, N., Lehrer-Graiwer, J., Hsin, H., Fraser, A.G., Kamath, R.S., Ahringer, J., and Kenyon, C. (2002). Rates of behavior and aging specified by mitochondrial function during development. Science *298*, 2398–2401.
26. Yang, W., and Hekimi, S. (2010). Two modes of mitochondrial dysfunction lead independently to lifespan extension in *Caenorhabditis elegans*. Aging Cell *9*, 433–447.
27. Rea, S.L., Ventura, N., and Johnson, T.E. (2007). Relationship between mitochondrial electron transport chain dysfunction, development, and life extension in *Caenorhabditis elegans*. PLoS Biol. *5*, e259.
28. Mangone, M., Manoharan, A.P., Thierry-Mieg, D., Thierry-Mieg, J., Han, T., Mackowiak, S.D., Mis, E., Zegar, C., Gutwein, M.R., Khivansara, V., et al. (2010). The landscape of C. elegans 3¢UTRs. Science *329*, 432–435.
29. Fillingham, J., Kainth, P., Lambert, J.-P., van Bakel, H., Tsui, K., Peña-Castillo, L., Nislow, C., Figeys, D., Hughes, T.R., Greenblatt, J., and Andrews, B.J. (2009). Two-color cell array screen reveals interdependent roles for histone chaperones and a chromatin boundary regulator in histone gene repression. Mol. Cell *35*, 340–351.
30. Mitchell, A.L., Attwood, T.K., Babbitt, P.C., Blum, M., Bork, P., Bridge, A., Brown, S.D., Chang, H.Y., El-Gebali, S., Fraser, M.I., et al. (2019). InterPro in 2019: improving coverage, classification and access to protein sequence annotations. Nucleic Acids Res. *47* (D1), D351–D360.
31. Ricketts, M.D., Frederick, B., Hoff, H., Tang, Y., Schultz, D.C., Singh Rai, T., Grazia Vizioli, M., Adams, P.D., and Marmorstein, R. (2015). Ubinuclein-1 confers histone H3.3-specific-binding by the HIRA histone chaperone complex. Nat. Commun. *6*, 7711.

32. Schneiderman, J.I., Orsi, G.A., Hughes, K.T., Loppin, B., and Ahmad, K. (2012). Nucleosome-depleted chromatin gaps recruit assembly factors for the H3.3 histone variant. Proc. Natl. Acad. Sci. USA *109*, 19721–19726.

33. Iwase, S., Xiang, B., Ghosh, S., Ren, T., Lewis, P.W., Cochrane, J.C., Allis, C.D., Picketts, D.J., Patel, D.J., Li, H., and Shi, Y. (2011). ATRX ADD domain links an atypical histone methylation recognition mechanism to human mental-retardation syndrome. Nat. Struct. Mol. Biol. *18*, 769–776.

34. Ooi, S.L., Priess, J.R., and Henikoff, S. (2006). Histone H3.3 variant dynamics in the germline of *Caenorhabditis elegans*. PLoS Genet. *2*, e97.

35. Sakai, A., Schwartz, B.E., Goldstein, S., and Ahmad, K. (2009). Transcriptional and developmental functions of the H3.3 histone variant in *Drosophila*. Curr. Biol. *19*, 1816–1820.

36. Ferguson, E.L., and Horvitz, H.R. (1989). The multivulva phenotype of certain *Caenorhabditis elegans* mutants results from defects in two functionally redundant pathways. Genetics *123*, 109–121.

37. Lakowski, B., and Hekimi, S. (1996). Determination of life-span in *Caenorhabditis elegans* by four clock genes. Science *272*, 1010–1013.

38. Boycott, A.E., Diver, C., Garstang, S.L., and Turner, F.M. (1931). II. The inheritance of sinistrality in Limnæa peregra (Mollusca, Pulmonata). Philos. Trans. R. Soc. Lond. Ser. B Contain. Pap. Biol. Character *219*, 51–131.

39. Moravec, C.E., Samuel, J., Weng, W., Wood, I.C., and Sirotkin, H.I. (2016). Maternal Rest/Nrsf Regulates Zebrafish Behavior through *snap25a/b*. J. Neurosci. *36*, 9407–9419.

40. Wasson, J.A., Simon, A.K., Myrick, D.A., Wolf, G., Driscoll, S., Pfaff, S.L., Macfarlan, T.S., and Katz, D.J. (2016). Maternally provided LSD1/KDM1A enables the maternal-to-zygotic transition and prevents defects that manifest postnatally. eLife *5*, e08848.

41. Szenker, E., Lacoste, N., and Almouzni, G. (2012). A developmental requirement for HIRA-dependent H3.3 deposition revealed at gastrulation in *Xenopus*. Cell Rep. *1*, 730–740.

42. Kong, Q., Banaszynski, L.A., Geng, F., Zhang, X., Zhang, J., Zhang, H., O'Neill, C.L., Yan, P., Liu, Z., Shido, K., et al. (2018). Histone variant H3.3-mediated chromatin remodeling is essential for paternal genome activation in mouse preimplantation embryos. J. Biol. Chem. *293*, 3829–3838.

43. Inoue, A., and Zhang, Y. (2014). Nucleosome assembly is required for nuclear pore complex assembly in mouse zygotes. Nat. Struct. Mol. Biol. *21*, 609–616.

44. Elsässer, S.J., Noh, K.-M., Diaz, N., Allis, C.D., and Banaszynski, L.A. (2015). Histone H3.3 is required for endogenous retroviral element silencing in embryonic stem cells. Nature *522*, 240–244.

45. Banaszynski, L.A., Wen, D., Dewell, S., Whitcomb, S.J., Lin, M., Diaz, N., Elsässer, S.J., Chapgier, A., Goldberg, A.D., Canaani, E., et al. (2013). Hira-dependent histone H3.3 deposition facilitates PRC2 recruitment at developmental loci in ES cells. Cell *155*, 107–120.

46. Goldberg, A.D., Banaszynski, L.A., Noh, K.M., Lewis, P.W., Elsaesser, S.J., Stadler, S., Dewell, S., Law, M., Guo, X., Li, X., et al. (2010). Distinct factors control histone variant H3.3 localization at specific genomic regions. Cell *140*, 678–691.

47. Akiyama, T., Suzuki, O., Matsuda, J., and Aoki, F. (2011). Dynamic replacement of histone H3 variants reprograms epigenetic marks in early mouse embryos. PLoS Genet. *7*, e1002279.

48. Santenard, A., Ziegler-Birling, C., Koch, M., Tora, L., Bannister, A.J., and Torres-Padilla, M.-E. (2010). Heterochromatin formation in the mouse embryo requires critical residues of the histone variant H3.3. Nat. Cell Biol. *12*, 853–862.

49. Ng, R.K., and Gurdon, J.B. (2008). Epigenetic memory of an active gene state depends on histone H3.3 incorporation into chromatin in the absence of transcription. Nat. Cell Biol. *10*, 102–109.

50. Greer, E.L., Maures, T.J., Ucar, D., Hauswirth, A.G., Mancini, E., Lim, J.P., Benayoun, B.A., Shi, Y., and Brunet, A. (2011). Transgenerational epigenetic inheritance of longevity in *Caenorhabditis elegans*. Nature *479*, 365–371.

51. Lesch, B.J., Tothova, Z., Morgan, E.A., Liao, Z., Bronson, R.T., Ebert, B.L., and Page, D.C. (2019). Intergenerational epigenetic inheritance of cancer susceptibility in mammals. eLife *8*, e39380.

52. Kong, A., Thorleifsson, G., Frigge, M.L., Vilhjalmsson, B.J., Young, A.I., Thorgeirsson, T.E., Benonisdottir, S., Oddsson, A., Halldorsson, B.V., Masson, G., et al. (2018). The nature of nurture: Effects of parental genotypes. Science *359*, 424–428.

53. Brenner, S. (1974). The genetics of *Caenorhabditis elegans*. Genetics *77*, 71–94.

54. Zhang, D., Tu, S., Stubna, M., Wu, W.S., Huang, W.C., Weng, Z., and Lee, H.C. (2018). The piRNA targeting rules and the resistance to piRNA silencing in endogenous genes. Science *359*, 587–592.

55. Frøkjaer-Jensen, C., Davis, M.W., Hopkins, C.E., Newman, B.J., Thummel, J.M., Olesen, S.-P., Grunnet, M., and Jorgensen, E.M. (2008). Single-copy insertion of transgenes in *Caenorhabditis elegans*. Nat. Genet. *40*, 1375–1383.

56. Okkema, P.G., Harrison, S.W., Plunger, V., Aryana, A., and Fire, A. (1993). Sequence requirements for myosin gene expression and regulation in *Caenorhabditis elegans*. Genetics *135*, 385–404.

57. Mahoney, T.R., Liu, Q., Itoh, T., Luo, S., Hadwiger, G., Vincent, R., Wang, Z.-W., Fukuda, M., and Nonet, M.L. (2006). Regulation of synaptic transmission by RAB-3 and RAB-27 in *Caenorhabditis elegans*. Mol. Biol. Cell *17*, 2617–2625.

58. Allman, E., Johnson, D., and Nehrke, K. (2009). Loss of the apical V-ATPase a-subunit VHA-6 prevents acidification of the intestinal lumen during a rhythmic behavior in *C. elegans*. Am. J. Physiol. Cell Physiol. *297*, C1071–C1081.

59. Kennedy, B.P., Aamodt, E.J., Allen, F.L., Chung, M.A., Heschl, M.F.P., and McGhee, J.D. (1993). The gut esterase gene (ges-1) from the nematodes *Caenorhabditis elegans* and *Caenorhabditis briggsae*. J. Mol. Biol. *229*, 890–908.

60. Davis, M.W., Hammarlund, M., Harrach, T., Hullett, P., Olsen, S., and Jorgensen, E.M. (2005). Rapid single nucleotide polymorphism mapping in *C. elegans*. BMC Genomics *6*, 118.

61. Bhatla, N., Droste, R., Sando, S.R., Huang, A., and Horvitz, H.R. (2015). Distinct neural circuits control rhythm inhibition and spitting by the myogenic pharynx of *C. elegans*. Curr. Biol. *25*, 2075–2089.

62. Langmead, B., Trapnell, C., Pop, M., and Salzberg, S.L. (2009). Ultrafast and memory-efficient alignment of short DNA sequences to the human genome. Genome Biol. *10*, R25–R25.

63. Li, B., and Dewey, C.N. (2011). RSEM: accurate transcript quantification from RNA-Seq data with or without a reference genome. BMC Bioinformatics *12*, 323.

64. Li, H., Handsaker, B., Wysoker, A., Fennell, T., Ruan, J., Homer, N., Marth, G., Abecasis, G., and Durbin, R.; 1000 Genome Project Data Processing Subgroup (2009). The Sequence Alignment/Map format and SAMtools. Bioinformatics *25*, 2078–2079.

65. Anders, S., and Huber, W. (2010). Differential expression analysis for sequence count data. Genome Biol. *11*, R106.

STAR★METHODS

KEY RESOURCES TABLE

REAGENT or RESOURCE	SOURCE	IDENTIFIER
Antibodies		
Rabbit polyclonal anti-HIRA-1 (32915)	This paper	N/A
Rabbit polyclonal anti-HIRA-1 (39216)	This paper	N/A
Bacterial and Virus Strains		
E. coli: OP50	*Caenorhabditis* Genetics Center	RRID: WB-STRAIN:OP50-1
Chemicals, Peptides, and Recombinant Proteins		
TRIzol Reagent	ThermoFisher Scientific	Cat#15596018
Chemical: Ethyl methanesulfonate	Sigma-Aldrich	Cat#M0880
Critical Commercial Assays		
In-Fusion HD Cloning System	TaKaRa	Cat#639637
Recombinant DNA		
Plasmid: $P_{hira\text{-}1}$::mcherry^{dpiRNA}::hira-1::hira-1 3'UTR	This paper	N/A
Plasmid: $P_{myo\text{-}3}$::mcherry::F2A::hira-1 cDNA::tbb-2 3'UTR	This paper	N/A
Plasmid: $P_{rab\text{-}3}$::mcherry::F2A::hira-1 cDNA::tbb-2 3'UTR	This paper	N/A
Plasmid: $P_{vha\text{-}6}$::mcherry::F2A::hira-1 cDNA::tbb-2 3'UTR	This paper	N/A
Plasmid: $P_{myo\text{-}3}$::3xFLAG::hira-1::tbb-2 3'UTR	This paper	N/A
Plasmid: $P_{rab\text{-}3}$::3xFLAGhira-1::tbb-2 3'UTR	This paper	N/A
Plasmid: $P_{ges\text{-}1}$::3xFLAG::hira-1::tbb-2 3'UTR	This paper	N/A
Deposited Data		
RNA-seq data	This paper	GEO: GSE144686
Experimental Models: Organisms/Strains		
C. elegans	This paper	Table S2
Software and Algorithms		
ImageJ	NIH image	RRID: SCR_003070
GraphPad Prism	GraphPad	RRID: SCR_002798
Zen	Zeiss	https://www.zeiss.com/microscopy/us/downloads/zen.html

RESOURCE AVAILABILITY

Lead Contact

Further information and requests for reagents should be directed to and will be fulfilled by the Lead Contact, H. Robert Horvitz (horvitz@mit.edu).

Materials Availability

All unique/stable reagents generated in this study are available from the Lead Contact without restriction.

Data and Code Availability

The accession number for the RNA-seq data reported in this paper is GEO: GSE144686.

EXPERIMENTAL MODEL AND SUBJECT DETAILS

C. elegans strains used in this study are listed in Table S2. Strains were maintained at 20°C on Nematode Growth Medium plates containing 3 g/L NaCl, 2.5 g/L peptone and 17 g/L agar supplemented with 1 mM $CaCl_2$, 1 mM $MgSO_4$, 1 mM KPO_4 and 5 mg/L cholesterol with *E. coli* OP50 as a source of food [53]. *hira-1(–)* indicates *hira-1(gk835598)*. All measurements were taken from hermaphrodite animals.

METHOD DETAILS

Microscopy

Bright field, Nomarski differential interference contrast (DIC) and epifluorescence images were obtained using Axio Imager.Z2 (Zeiss) and LSM 800 (Zeiss) microscopes. Images were processed using FIJI (NIH) and Photoshop (Adobe).

Plasmid and transgenic strain construction

***Transgene* nSi48: P_{hira-1}::mcherry^{dpiRNA}::hira-1::hira-1 3'UTR**

In-Fusion HD Cloning Kit (Takara) was used to fuse the following PCR products: P_{hira-1} (1003 bp directly 5'of *hira-1* ATG), *mcherry*^{dpiRNA} (lacks piRNA target sites to avoid transgene silencing in the germline [54]), *hira-1* gene (includes introns and 3' UTR, 4928 bp), pCJF350 MosSci plasmid targeting ttTi5605 (insertion site on chromosome II). This construct was injected at 10 ng/μl and integrated into chromosome II using MosSci [55].

***Transgene* nEx2902: P_{myo-3}::mcherry::F2A::hira-1 cDNA::tbb-2 3'UTR**

In-Fusion HD Cloning Kit (Takara) was used to fuse the following PCR products: P_{myo-3} [56], *mcherry* (from pCFJ104, www.wormbuilder.org), *hira-1 cDNA*, *tbb-2* 3' UTR (from pCFJ420, www.wormbuilder.org). This construct was injected at 20 ng/μl concentration with co-injection marker pCFJ420 (10 ng/μl, www.wormbuilder.org).

***Transgene* nEx2892: P_{rab-3}::mcherry::F2A::hira-1 cDNA::tbb-2 3'UTR**

In-Fusion HD Cloning Kit (Takara) was used to fuse the following PCR products: P_{rab-3} [57], *mcherry* (from pCFJ104, www.wormbuilder.org), *hira-1 cDNA*, *tbb-2* 3' UTR (from pCFJ420, www.wormbuilder.org). This construct was injected at 20 ng/μl concentration.

***Transgene* nEx2897: P_{vha-6}::mcherry::F2A::hira-1 cDNA::tbb-2 3'UTR**

In-Fusion HD Cloning Kit (Takara) was used to fuse the following PCR products: P_{vha-6} [58], *mcherry* (from pCFJ104, www.wormbuilder.org), *hira-1 cDNA*, *tbb-2* 3' UTR (from pCFJ420, www.wormbuilder.org). This construct was injected at 20 ng/μl concentration with co-injection marker pCFJ420: P_{eft-3}*::h2b::gfp* (10 ng/μl, www.wormbuilder.org).

***Transgene* nSi28: P_{myo-3}::3xFLAG::hira-1::tbb-2 3'UTR**

In-Fusion HD Cloning Kit (Takara) was used to fuse the following PCR products: P_{myo-3} [56], 3x FLAG, *hira-1* gene (includes introns), *tbb-2* 3' UTR (from pCFJ420, www.wormbuilder.org), pCJF350 MosSci plasmid targeting ttTi5605 (insertion site on chromosome II). This construct was injected at 10 ng/μl and integrated into chromosome II using MosSci [55].

***Transgene* nSi23: P_{rab-3}::3xFLAGhira-1::tbb-2 3'UTR**

In-Fusion HD Cloning Kit (Takara) was used to fuse the following PCR products: P_{rab-3} [57], 3xFLAG, *hira-1* gene (includes introns), *tbb-2* 3' UTR (from pCFJ420, www.wormbuilder.org), pCJF350 MosSci plasmid targeting ttTi5605 (insertion site on chromosome II). This construct was injected at 10 ng/μl and integrated into chromosome II using MosSci [55].

***Transgene* nSi21: P_{ges-1}::3xFLAG::hira-1::tbb-2 3'UTR**

In-Fusion HD Cloning Kit (Takara) was used to fuse the following PCR products: P_{ges-1} [59], 3x FLAG, *hira-1* gene (includes introns), *tbb-2* 3' UTR (from pCFJ420, www.wormbuilder.org), pCJF350 MosSci plasmid targeting oxTi185 (insertion site on chromosome I). This construct was injected at 10 ng/μl and integrated into chromosome II using MosSci [55].

Defecation

The enteric muscle contraction (EMC) that executes the expulsion step of the defecation motor program was observed using a dissecting microscope. The fraction of EMCs per five cycles per worm was measured.

Genetic screen and mutation identification

SJ4100 L4 larvae were mutagenized as described previously [53]. F3 animals were chosen based on three defects exhibited by *hira-1* mutants: small, pale, and misexpression of P_{hsp-6}*::gfp.* Mutants were backcrossed, mutations were mapped using SNP mapping [60], and genomic DNA from mutant isolates was analyzed by whole-genome sequencing.

Pharyngeal pumping

Two distinct pharyngeal behaviors were measured: feeding pumps, which occur when animals are left undisturbed in the presence of food (t = 0 to t = 10), and spitting pumps, which occur as a response to noxious 365 nm light [61].

Antibody production

Two anti-HIRA-1 antibodies were generated by Pocono Rabbit Farm and Laboratory (32915 and 32916). The three peptide sequences KSMEDNSKENESKNSEK, PALRPMEPKSLKTQEGT, and EAPEQQPKLSQHVVDRK (Figure 1B indicates location of peptides) were injected. Antisera were collected from two rabbits, and antibodies were affinity purified.

RNA-Seq

Total RNA was isolated using TRIzol Reagent (Thermo Fisher Scientific). mRNA was purified by polyA-tail enrichment, fragmented, and reverse transcribed into cDNA (Illumina TruSeq). cDNA samples were then end-repaired, adaptor-ligated using the SPRI-works Fragment Library System I (Beckman Coulter Genomics) and indexed during amplification. Libraries were quantified using the

Fragment Analyzer (Advanced Analytical) and qPCR before being loaded for paired-end sequencing using the Illumina NextSeq sequencer. RNA-seq data were aligned and summarized using bowtie version 1.0.1 [62], RSEM version 1.2.15 [63], samtools/0.1.19 [64] and a UCSC known genes annotation file from the ce10 assembly. Differential expression analysis was done with R version 2.15.3 using DESeq_1.10.1 [65]. For the genes and fold changes reported in Figures 4 and S4, our cutoff was an average of at least 5 FPKM (fragments per kilobase of transcript per million mapped reads) per gene, applied to each genotype independently. The p value cutoffs reported for the fold changes in Figures 4 and S4 were calculated using DESeq and take into account multiple testing.

Quantification of body size and pigmentation

Micrographs of whole worms were analyzed using FIJI. The perimeter was traced around each individual worm. The area within the perimeter was calculated and used to define the body size of each worm. The pixel intensity was also determined for the area inside the perimeter traced for each worm. For the calculation of pixel intensities, the pixel intensities of original micrographs were inverted. For example, the wild-type strain has darker pigmentation and when inverted has a higher value for pixel intensity. The background (selected from an arbitrary area of the micrograph that did not contain worms) from each image was subtracted from each measurement of pixel intensity.

QUANTIFICATION AND STATISTICAL ANALYSIS

For all quantification error bars represent standard deviation (SD). Student's t tests were used to determine statistical significance. Graphs and indicated statistical analyses were performed using Microsoft Excel and GraphPad Prism 7 software.